INTERNATIONAL JOURNAL FOR NUMERICAL METHODS IN FLUIDS, VOL. 3, 179–200 (1983)

NUMERICAL ANALYSIS OF A MOVING BOUNDARY PROBLEM IN COASTAL HYDRODYNAMICS

T. C. GOPALAKRISHNAN*

Department of Marine, Earth and Atmospheric Sciences, North Carolina State University, P.O. Box 5068, Raleigh, North Carolina 27650, U.S.A.

C. C. TUNG†

Department of Civil Engineering, North Carolina State University, P.O. Box 5993, Raleigh, North Carolina 27650, U.S.A.

SUMMARY

A finite element model to tackle the moving boundary problem of wave run-up on moderately steep slopes is developed. The special aspects considered in this study are (1) the modification of shallow water equations to accommodate the effect of vertical accelerations and (2) the use of Lagrangian acceleration coupled with an element that adapts itself to the moving boundary closely. The pressure term in the one-dimensional momentum equation is derived using the Eulerian equation in the vertical direction. This takes care of the vertical accelerations which are significant during the motion of a wave on moderately steep slopes. The element near the boundary is allowed to change its dimension so that the fluid boundary is closely followed. Such a flexible element precludes the need for approximation of the variables with regard to the indefinite position of the boundary. This element is split into two when its dimension becomes unduly large compared to the unchanging elements. The need for such a splitting is shown by an examination of the entries in the global matrix. Results of water profile as a wave runs up a structure are given. A brief history of the work on similar problems is outlined.

KEY WORDS Wave Run-up Hydrodynamics Moving-boundary Finite-element Model

1. INTRODUCTION

Many problems in fluid mechanics are characterized by moving boundaries. These problems present interesting features while applying numerical techniques. The adaptability of the finite element method to such problems arises from its capacity to handle curved boundaries and variable spatial discretization without complicating the solution procedure. The finite difference method has also been successfully applied to those problems. Most of the earlier works in connection with moving boundary phenomena used fixed grids. Those approaches tackled the moving boundary by alternatively including and excluding finite difference cells (or finite elements) at the boundary to deal with the varying domain; for example, Reid and Bodine,[32] Leendertse,[20] Holtz and Withum,[17] Nakano[26] and Xanthopoulos and Koutitas.[41] In recent years, however, continuously deforming finite difference grid or 'mobile' elements have been incorporated in the solution system; Boris *et al.*,[6] Jamet and Bonnerot,[19] Lynch and Gray,[21] Varoglu and Finn[37] and Gopalakrishnan and Tung[15] explain such a procedure.

* Assistant Professor and currently with the Kuwait Institute for Scientific Research, Kuwait.
† Professor

0271–2091/83/020179–22$02.20

Received 8 June 1981
Revised 1 April 1982

Yeh and Chou[43] describe a finite difference model which they refer to as 'discrete moving boundary' simulation. An interesting discussion on their work by Lynch can be found in Reference 22.

France[14] shows that, in certain cases, the fixed element grid is preferable (while effectively tackling the moving boundary) as it strikes considerable economy in computation. However, the conclusions hold good only for certain problems and their generalization is difficult especially for situations where the extent of boundary movement is comparable to that of the original domain.

Review articles on the numerical analysis of moving boundary problems are available in References 9, 13, 24 and 33. Recently Lynch and Gray[21] have presented an interesting summary of the investigations conducted in the last few years. An overview of moving boundary problems is sketched by Boley.[3]

In the area of finite element applications there are essentially two approaches: one is to use finite elements in both space and time and the other, the 'semi-discrete' method, namely finite elements in space and finite difference in the time domain. Bonnerot and Jamet[4,5] and Rushchak[34] have adopted the former while the latter is used by Mori,[25] Lynch and Gray[21] and Gopalakrishnan and Tung.[15]

Most of the deforming-grid techniques tentatively assume a position for the free surface and subsequently correct it by using an iterative procedure until the boundary conditions are satisfied to the desired degree of accuracy. However, some of the investigators have attempted to follow the boundary closely by using velocity and acceleration vectors of the fluid at the boundary.[15,21,23] The present paper describes the latter technique but the emphasis is on the splitting of the elements near the boundary as they become 'unwieldy' and on the introduction of the effects of vertical accelerations in the one-dimensional shallow water equations. Yeh and Chou[44] correctly point out the difficulties that may arise as a result of the elements at the boundary becoming very large. The present authors anticipated such a possibility and have incorporated a simple technique to overcome the difficulties.

The problem addressed to in this study is the wave run-up on beaches or structures of moderately steep slopes, such as 1 on 5. On flatter slopes the vertical accelerations can be ignored whereas very steep slopes will necessitate a two-dimensional resolution in the vertical plane.

An important aspect of the wave uprush problem is the wave breaking. In the present study only non-breaking waves are considered because the waves are known to climb the beach without breaking when the slopes are moderately steep. Attempts to include breaking are being made so that the moving boundary numerical model developed here can be applied to motion over flat slopes too, as is, indeed, the case when a storm surge rushes inland. Heitner and Housner[16] and Jamet and Bonnerot,[19] among others, show how a pseudo-viscosity term can be used to tackle such 'shock' conditions. Recently, Walton and Christensen[38] have offered a study of friction factors to be used in the motion of storm surge over coastal areas.

The present study uses the Galerkin finite element procedure to evaluate the time derivatives of velocity and water level in the varying problem domain of the wave run-up problem. Using these derivatives the variables are advanced in time via the Euler predictor–corrector scheme. The verification of the numerical model and its engineering significance have already been published by the authors;[15] as mentioned earlier, this paper concentrates on the governing equations and on the mobile element that is used to tackle the moving boundary. However, some of the material in the above mentioned publication is repeated here for completeness sake.

2. THE PHYSICAL PROBLEM

Waves approaching a shore are influenced by the bottom topography. Although the wave period remains unaltered, the wave height, length and celerity are modified by the varying depth of water. The particle velocities and the water levels are accordingly affected. This is the wave shoaling problem.

As the wave moves on the shoaling region it continuously builds up in height and eventually breaks when the depth of water is too shallow to support the wave height. This gives rise to a bore which then propagates and runs up the beach or structure as the case may be. Once a bore is formed the motion is no longer oscillatory. Under certain circumstances the wave may reach and run-up the beach or structure without breaking. The run-up problem is thus characterized by either a bore or a wave moving on a region not occupied by water initially.

Figure 1 depicts a vertical section through the near shore region and the beach, along the x-axis. The forcing function at $x = 0$ may be one of several kinds depending on whether the wave is solitary, cnoidal or sinusoidal. It can also be a bore if the wave breaks prior to reaching the plane $x = 0$.

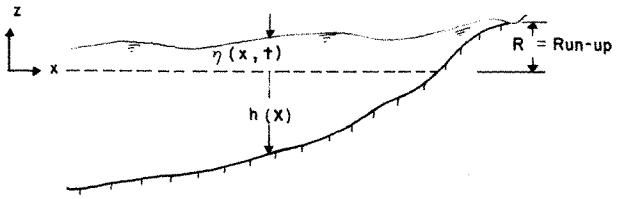

Figure 1. Wave shoaling and run-up

The objective of the study is to compute the water profile $\eta(x, t)$ and the mean velocity $U(x, t)$ for a given beach configuration and forcing function.

The flow in the region under consideration is assumed to be inviscid and incompressible. The density of water ρ and the atmospheric pressure remain constant. The effect of wind, percolation, Coriolis and tide generating forces are neglected. Currents are not present and the forcing wave is assumed to enter still water conditions.

3. THEORY

The starting point of this investigation is the Eulerian equations of motion in two dimensions. The Cartesian axes x and z are taken along the horizontal and vertical directions, respectively (Figure 1); the corresponding components of velocity are u and w. Pressure is represented by p. Thus

$$u = u(x, z, t)$$

$$w = w(x, z, t)$$

$$p = p(x, z, t)$$

in which t is time. When gravity is the only body force considered, the following momentum

equations result:

$$\frac{\partial u}{\partial t}+u\frac{\partial u}{\partial x}+w\frac{\partial u}{\partial z}=-\frac{1}{\rho}\frac{\partial \rho}{\partial x} \tag{1}$$

$$\frac{\partial w}{\partial t}+u\frac{\partial w}{\partial x}+w\frac{\partial w}{\partial z}=-\frac{1}{\rho}\frac{\partial \rho}{\partial z}-g \tag{2}$$

where g is the acceleration due to gravity.

The continuity equation is:

$$\frac{\partial u}{\partial x}+\frac{\partial w}{\partial z}=0 \tag{3}$$

When developing the shallow water equations, the term $(1/\rho)(\partial p/\partial x)$ is replaced by $g(\partial \eta/\partial x)$ based on the hydrostatic pressure assumption. However, when vertical accelerations can be considerable such an assumption will not hold good. The problem of wave shoaling and run-up usually involves considerable vertical accelerations. An attempt is made here to approximately evaluate the vertical accelerations in terms of the one-dimensional velocity U, water level η and the bottom slope $\partial h/\partial x$. With the introduction of vertical accelerations the one-dimensional momentum equation can be considered as a 'quasi two-dimensional' equation.

The terms which account for vertical accelerations in the momentum equation are derived from considerations of pressure variation on a vertical section. An expression for this variation can be obtained from the momentum equation for the z-direction, equation (2). Once this variation is established the corresponding effect can be introduced in the term $-(1/\rho)(\partial p/\partial x)$ of the momentum equation for the x-direction, equation (1). Thus, we obtain an equation for the x-direction in which the effects of vertical accelerations are included. The following paragraphs explain the steps involved in arriving at the modified 1-D (or the quasi 2-D) equation. In the initial stages this development follows that of Peregrine.[30]

The x-component of the particle velocity can be represented by a mean and fluctuating terms as

$$u(x, z, t)=U(x, t)+u^*(x, z, t) \tag{4}$$

where

$$\int_{-h}^{\eta} u^* \,\mathrm{d}z=0 \quad \text{and} \quad U(x, t)=\frac{1}{h+\eta}\int_{-h}^{\eta} u(x, z, t)\,\mathrm{d}z$$

Based on this relationship, equation (1) becomes

$$\frac{\partial(U+u^*)}{\partial t}+(U+u^*)\frac{\partial(U+u^*)}{\partial x}+w\frac{\partial(U+u^*)}{\partial z}=-\frac{1}{\rho}\frac{\partial \rho}{\partial x} \tag{5}$$

At this stage it is assumed that u^* is negligible compared to U, i.e. the horizontal velocity is assumed to be uniform over a vertical section. This assumption has been found to introduce negligible errors in most shallow water motions. Expanding the terms in equation (5) and neglecting small quantities gives

$$\frac{\partial U}{\partial t}+U\frac{\partial U}{\partial x}=-\frac{1}{\rho}\frac{\partial p}{\partial x} \tag{6}$$

which, when integrated over z yields

$$(\eta+h)\left(\frac{\partial U}{\partial t}+U\frac{\partial U}{\partial x}\right)=-\frac{1}{\rho}\int_{-h}^{\eta}\frac{\partial p}{\partial x}\,\mathrm{d}z \tag{7}$$

the vertically-averaged horizontal momentum equation.

Similarly, the vertical momentum equation (2) can be approximated by

$$\frac{\partial w}{\partial t}+U\frac{\partial w}{\partial x}+w\frac{\partial w}{\partial z}=-\frac{1}{\rho}\frac{\partial p}{\partial z}-g \tag{8}$$

and the continuity equation (3) by

$$\frac{\partial w}{\partial z}=-\frac{\partial U}{\partial x} \tag{9}$$

Since the right-hand side of equation (9) is only a function of x and t, it follows that in this approximation w is at most a linear function of z. Thus, using the boundary condition that

$$w=-(U+u^*)\frac{\partial h}{\partial x}\simeq -U\frac{\partial h}{\partial x} \quad \text{at} \quad z=-h,$$

equation (9) can be integrated to give

$$w=-\frac{\partial U}{\partial x}z-\frac{\partial}{\partial x}(Uh) \tag{10}$$

as an approximation to the true vertical velocity. Based on this, the various terms on the left-hand side of the approximate vertical momentum equation (8) can be explicitly evaluated, giving

$$\left.\begin{aligned}\frac{\partial w}{\partial t}&=-z\frac{\partial^2 U}{\partial x\,\partial t}-\frac{\partial}{\partial x}\left(h\frac{\partial U}{\partial t}\right)\\ \frac{\partial w}{\partial x}&=-z\frac{\partial^2 U}{\partial x^2}-\left[U\frac{\partial^2 h}{\partial x^2}+2\frac{\partial U}{\partial x}\frac{\partial h}{\partial x}+h\frac{\partial^2 u}{\partial x^2}\right]\end{aligned}\right\} \tag{11}$$

and equation (9).

Thus, the left hand side of equation (8) can be expressed as a function ζ of U and its time and space derivatives, h and its space derivatives and z, i.e. equation (8) can now be written as

$$\zeta\left(U, h, \frac{\partial U}{\partial x}, \frac{\partial h}{\partial x}, \frac{\partial^2 U}{\partial x^2}, \frac{\partial^2 h}{\partial x^2}, \frac{\partial U}{\partial t}, z\right)=-\frac{1}{\rho}\frac{\partial \rho}{\partial z}-g \tag{12}$$

Integrating equation (12) with regard to z yields

$$-\frac{p}{\rho}=g(z-\eta)+\int_z^\eta \zeta(x, \bar{z}, t)\,d\bar{z} \tag{13}$$

where $p=0$ at $z=\eta$ has been utilized. Differentiating equation (13) with respect to x gives

$$-\frac{1}{\rho}\frac{\partial p}{\partial x}=-g\frac{\partial \eta}{\partial x}+\int_z^\eta \frac{\partial \zeta}{\partial x}(x, \bar{z}, t)\,d\bar{z}+\zeta(x, \eta, t)\frac{\partial \eta}{\partial x} \tag{14}$$

which can now be inserted into the horizontal momentum equation (7) to give

$$\frac{\partial U}{\partial t}+U\frac{\partial U}{\partial x}+g\frac{\partial \eta}{\partial x}=\frac{1}{\eta+h}\int_{-h}^{\eta}\left[\int_z^\eta \frac{\partial \zeta}{\partial x}(x, \bar{z}, t)\,d\bar{z}\right]dz+\zeta(x, \eta, t)\frac{\partial \eta}{\partial x} \tag{15}$$

Comparing equation (15) with the well known shallow water momentum equation, it is seen that the (approximate) effect of vertical motion comes in through the terms on the right-hand

side of equation (15). Since U and h are not functions of z, these terms are easily evaluated explicitly. For example, the term $\frac{\partial w}{\partial t}$ (see equation (11)), which forms one of the terms (F_1) in the function ζ, gives:

$$-F_1 = \frac{1}{\eta+h}\int_{-h}^{\eta}\left[\int_z^{\eta}\left(\bar{z}\frac{\partial^3 U}{\partial x^2\,\partial t}+\frac{\partial^2}{\partial x^2}\left(h\frac{\partial U}{\partial t}\right)\right)d\bar{z}\right]dz+\left[\eta\frac{\partial^2 U}{\partial x\,\partial t}+\frac{\partial}{\partial x}\left(h\frac{\partial U}{\partial t}\right)\right]\frac{\partial \eta}{\partial x}$$

$$=\left[\tfrac{1}{2}\eta^2-\tfrac{1}{6}(\eta^2-\eta h+h^2)\right]\frac{\partial^3 U}{\partial x^2\,\partial t}+\left[\eta-\tfrac{1}{2}(\eta-h)\right]\frac{\partial^2}{\partial x^2}\left(h\frac{\partial U}{\partial t}\right) \tag{16}$$

$$+\left[\eta\frac{\partial^2 U}{\partial x\,\partial t}+\frac{\partial}{\partial x}\left(h\frac{\partial U}{\partial t}\right)\right]\frac{\partial \eta}{\partial x}$$

Equation (15) is then the 1-D momentum equation which accounts for vertical accelerations and hence may be called the 'quasi 2-D equation'. It is evident from the above development of the quasi 2-D momentum equation that the consideration of vertical accelerations does not affect the form of the 1-D continuity equation, i.e. equation (3) can be averaged over z to arrive at the well known exact shallow water continuity equation, namely

$$\frac{\partial \eta}{\partial t}+\frac{\partial}{\partial x}[U(\eta+h)]=0 \tag{17}$$

(Note: The use of both the exact and approximate (e.g. equation (10)) continuity equations in the derivation is consistent with the assumption that $u^* \ll U$.) Thus, equations (15) and (17) constitute the set of equations to be used for the shoaling and run-up problems in the quasi 2-D system. Effects of bottom friction can now be introduced via concepts of drag. Details of this are given in reference 15.

Initial and boundary conditions

Still water conditions are assumed at the initial instant $t=0$. Therefore,

$$\left.\begin{aligned} U(x,0)&=0\\ \eta(x,0)&=0\end{aligned}\right\} \quad \text{for all } x\geq 0$$

The point $x=0$ is referred to as the upstream point in this study. The tip of the moving front on the beach is the downstream point. The upstream boundary condition is provided by the forcing function as explained in the previous section. From the expression for η describing such functions the rate of change of water level at the upstream point can be obtained. At the downstream side the value of η depends on the velocity of the tip of moving water and the beach slope. The imposition of the downstream boundary condition is associated with the moving boundary aspect of the problem and will be explained in detail in a later section. In short, it is noted that the upstream and downstream boundary conditions are supplied through the values of $\partial\eta/\partial t$ and U, respectively. The latter requires considerations of the Lagrangian acceleration and this forms the essential aspect of handling the moving boundary part of the problem.

The number of boundary conditions for a given problem depends on the number of equations in the mathematical system governing the physical situation and on the order of differential equations in that system. This is the case for problems of unchanging domain. However, for moving boundary problems, additional conditions are to be specified in order to follow the boundary as it moves. These additional conditions are not used to solve the

differential equations in the system but to prescribe the value of the variable on the boundary consistent with the motion. Such conditions may be termed consistency conditions. The number of consistency conditions will be equal to the number of directions in which the boundary is moving.

In the present model, the unknowns are two in number, namely U and η, and the corresponding mathematical system consists of two equations (15) and (17)). These equations are of the first order. Thus, we need two boundary conditions, namely, one on U and one on η, to solve the system. There are cases in which the one dimensional system of equations have been solved using η at both the upstream and downstream points even though one of the two equations is predominantly with regard to U. This approach is admissible but the accuracy of the results depends on how strongly the two equations are coupled. However, in the present study one condition on η and one on U are used. Thus, the problem is mathematically 'well posed'.

The number of 'consistency conditions' in order to follow the moving boundary (in the present one-dimensional system) is 1 because the boundary expands or contracts (along the x-axis) at the downstream side only. This consistency condition is supplied through η at the downstream point as explained in a later section.

4. THE NUMERICAL MODEL

In order to solve the governing partial differential equations numerically, the Galerkin finite element procedure is adopted. Several works published in recent years exemplify the usefulness and power of this approach in fluid flow analysis. In general, a space–time dependent problem requires discretization both in space and time. Such a combined discretization leads to large implicit systems of equations. It is known that in the case of hyperbolic problems the implicit finite element systems are cumbersome to handle.[12] In the present study, the finite element procedure is adopted for spatial resolution only. This results in a solution system that yields the time derivatives of the variables. The time integration is performed using the Euler predictor–corrector scheme.

The variables U and η being one-dimensional in the current study, the discretization is with line elements, as shown in Fig. 2. It is seen that the whole domain is not discretized at the beginning because the equations are applicable only up to the point to which the water body extends. The manner of keeping up with the moving boundary and having the last node E always at the tip of water form the second salient feature of the present model, the first being the non-hydrostatic approximation.

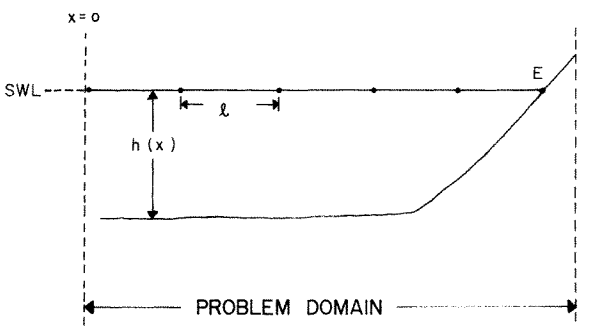

Figure 2. Spatial discretization

Choice of shape function

The Hermitian cubic shape function is eminently suited to the situation analysed herein. Moreover, being a cubic polynomial it can adapt itself to the 'corrugations' on the water surface that occur as water starts moving up the beach. These corrugations are actually the mild shocks that travel upstream from the front, as the leading edge of water traverses a dry bottom. The present study considers only non-breaking waves, but mild shocks are still possible and should be accommodated.

While following the moving tip of the water front, it is necessary to use the Lagrangian acceleration of that point. This requires the spatial gradient of U. One of the advantages of using the Hermitian cubic shape function is that such a gradient is obtained as part of the solution, precluding thereby the need to compute it explicitly. Moreover, the inclusion of vertical acceleration effects necessitate dealing with spatial derivatives through third order which is facilitated using cubic shape functions.

The solution system

Based on the above numerical technique, the governing partial differential equations issue two matrix equations as shown below:

$$[C_1]\{\dot{U}\} = \{b_1\}$$

$$[C_2]\{\dot{\eta}\} = \{b_2\}$$

where the dot notation stands for the time derivative. Solution of these equations produces the time derivatives of U and η at the nodes. The time integration scheme to obtain the time history of the variables is explained below.

5. TIME INTEGRATION

In order to reduce the error due to the use of constant rates of change of η and U within the time step, an iterative procedure is necessary. This is introduced in the time integration via the predictor–corrector technique. The simplest of such techniques (the Euler predictor–corrector) is the one that takes into account the rates of change at two successive instants. The predicted value for the next instant considers the gradient at the present instant. This enables us to compute the approximate gradient at the next instant. The corrected value is then obtained using the mean of the two gradients mentioned above. The iterations are repeated until two successive corrected values for the next instant agree within a limit. Higher order predictor–correctors, such as the Adams–Moulton method, consider the rates of change at more than two instants. However, the convergence rates will be slower in general. In the problem of run-up the number of time steps to be executed can be very large. Therefore, in order to strike a compromise between high accuracy and rapid convergence, the Euler predictor–corrector was chosen for this study.

The moving boundary aspect

In many hydrodynamic phenomena the problem domain is such that the boundaries or control sections do not change with time; for example, problems involving flood routing. If the free surface is considered as a boundary, then flood routing will also come under moving boundary problems. But in most cases of flood routing, one-dimensional models have been

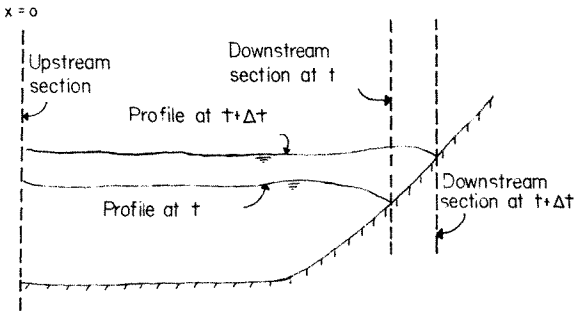

Figure 3. The moving downstream section

adopted and those imply that the free surface is implicitly included in the continuity equation. Hence, in the one-dimensional approaches the free surface is not considered a boundary of the problem domain. In fact, being one-dimensional the variables depend only on x and only in this direction need the boundaries be specified. The flood routing problem has thus an upstream and downstream boundary which remain fixed in time. The wave shoaling problem is very similar to flood routing and hence, in the one-dimensional system, it too is not a moving boundary problem. However, the wave run-up problem, even in the one-dimensional approximation, differs from flood routing and shoaling problems in that it has a moving problem domain.

The wave run-up problem has an upstream control section, i.e. the vertical plane $x=0$ (Figure 3) and a downstream control section at the tip of the wedge of water on the sloping beach. The upstream section remains unchanged in time. However, the downstream section must move with the water front because the tip of the moving front changes its position on the beach with time. This is what characterizes wave run-up as a moving boundary problem.

Let it be assumed that at time t the wave has reached the shore line and is about to climb the beach as in Figure 4. The last element (or the end element) denoted as AB has a length l

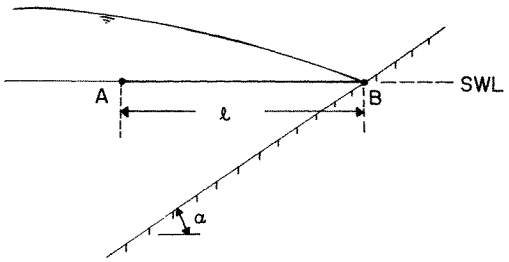

Figure 4. Water profile and end-element at time t.

at time t. At time $(t+\Delta t)$ the tip of water has moved up (Figure 5). We let the last node move with the tip and take up the position B_1 at $(t+\Delta t)$. The end-element length now is l_1, as shown in Figure 5. In order to determine l_1, we should consider the Lagrangian motion of water at the tip of the moving front. This is so because at this point we are moving with the particle. The distance s which is equal to l_1-l is given by

$$s = U_e(t)(\Delta t)+\tfrac{1}{2}a(\Delta t)^2$$

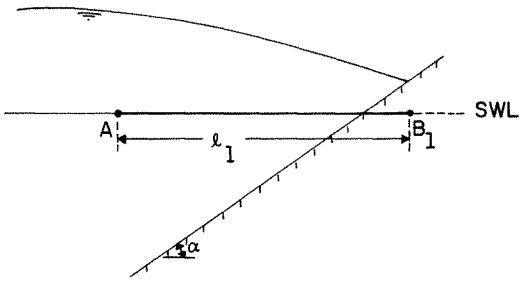

Figure 5. Water profile and end-element at time $t+\Delta t$

where $U_e(t)$ is the velocity of the tip at time t and a is the Lagrangian acceleration, assumed constant in the interval Δt; i.e. the sum of local and convective accelerations. Equivalently, $\dot{s} = U_e$ and $\dot{U}_e = a$, and the above expression for s is a second order accurate Taylor series approximation. The water level η at the tip of the front is $(s \tan \alpha)$ where α is the angle of the beach slope to the horizontal plane. However, a more accurate and numerically stable way of determining U and η at the tip, adopted in the present study, is explained below.

In the above approach, the end element has a length which is time dependent. Moreover, its length changes as the waves moves up or down the beach. If the end element has a length much larger than the elements prior to it then the global coefficient matrix will tend towards becoming ill-conditioned and the approximation will be poor in this element. In order to avoid this we split the end element into two elements when its length exceeds the 'regular' element length by a certain amount, say 20 per cent. This means that we are introducing a new node between the last two nodes. The values of the variable at the new node can be easily obtained by using the shape functions and the position of the new node between the last two nodes. This procedure is illustrated using Figures 6–8.

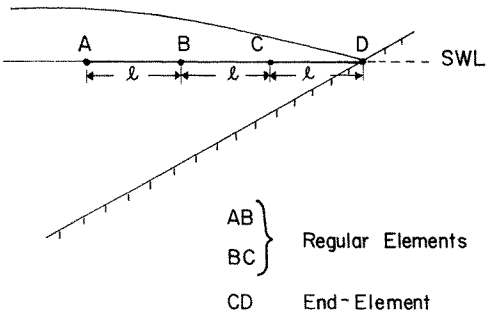

Figure 6. Position at time t

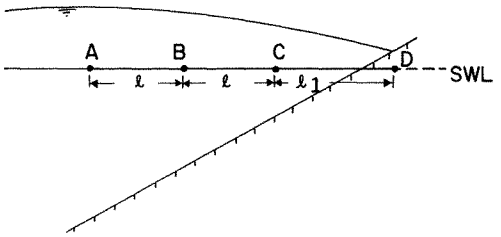

Figure 7. Position at time $t+\Delta t$

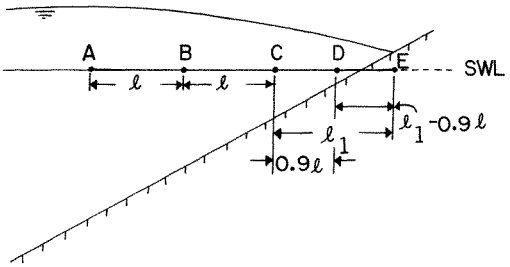

Figure 8. Element splitting at time $t+\Delta t$

After this step of splitting the end-element CD into the two elements CD and DE, the element CD remains constant in length and DE becomes the end-element with the node E now following the tip. By such a procedure we are able to have mobile elements at the end while avoiding the possibility of the coefficient matrix becoming ill-conditioned.

Determination of U and η at the moving tip

What dictates the flow on the downstream side is the ground slope and the velocity at the tip of the moving water. Let the velocity of water at the tip be U_e and the water level there be η_e. The continuum boundary conditions at the tip, $\eta = h$, are given by

$$\frac{d\eta_e}{dt} = U_e \frac{dh}{dx} = U_e \tan\alpha$$

and

$$\frac{dX_e}{dt} = U_e$$

where X_e is the location of the tip. These boundary conditions are similar to those adopted by Lynch and Gray[21] but the Lagrangian motion of the tip is obtained in a different manner. From Figure 9 it is seen that the tip travels a horizontal distance s in the interval Δt. The mean acceleration of the tip in the period between t and $t+\Delta t$ is

$$a_m = [a_e(t) + a_e(t+\Delta t)]/2 \tag{18}$$

Hence,

$$s = U_e \Delta t + a_m (\Delta t)^{\frac{21}{2}} \tag{19}$$

From the geometry of Figure 9 it follows that

$$\eta_e(t+\Delta t) = \eta_e(t) + s \tan\alpha \tag{20}$$

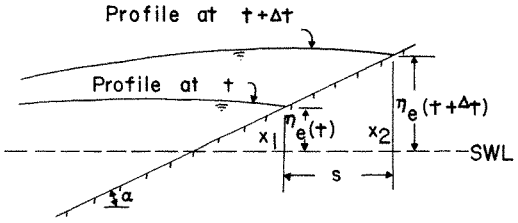

Figure 9. Downstream conditions at the instants t and $t+\Delta t$

However, it is seen above that in the computation of $\eta_e(t+\Delta t)$, $U_e(t+\Delta t)$ is involved and that $U_e(t+\Delta t)$ is unknown until all quantities for the instant $(t+\Delta t)$ have been computed. This difficulty is overcome in the process of applying the Euler predictor–corrector as detailed before. The following lines explain the steps involved in arriving at $\eta_e(t+\Delta t)$ and $U_e(t+\Delta t)$.

The value of the velocity $U_e(t+\Delta t)$ can be predicted by considering the Lagrangian acceleration of the tip. Let this acceleration be a at the instant t. Therefore,

$$U_e(t+\Delta t) = U_e(t) + a\Delta t \tag{21}$$

But a itself is a function of time. Hence, during the predictor–corrector operation adopted for moving ahead in time, the repeated iterations take the mean of the total accelerations $a(t)$ and $a(t+\Delta t)$ into account. The following steps explain the relationships during the iterations of predictor (superscript p) and corrector (superscript c):

Predictor operations.

$$a(t) = \frac{\partial U_e(t)}{\partial t} + U_e(t)\frac{\partial U_e(t)}{\partial x}$$

$$U_e^p(t+\Delta t) = U_e(t) + a(t)\Delta t$$

which is an approximation to the continuum equation

$$\frac{dU_e}{dt} = \frac{\partial U_e}{\partial t} + U_e\frac{\partial U_e}{\partial x}$$

the acceleration following the moving tip.

$$s^p = U_e(t)\Delta t + a(t)(\Delta t)^2\tfrac{1}{2}$$

$$\eta_e^p(t+\Delta t) = \eta_e(t) + s^p \tan\alpha$$

Using the above value of $U_e(t+\Delta t)$ as the downstream boundary condition and $\eta_e(t+\Delta t)$ as the consistency condition all quantities for the instant $(t+\Delta t)$ are computed.

Corrector operations.

$$a(t+\Delta t) = \frac{\partial U_e^p(t+\Delta t)}{\partial t} + U_e^p(t+\Delta t)\frac{\partial U_e^p(t+\Delta t)}{\partial x}$$

$$U_e^c(t+\Delta t) = U_e(t) + a_m\Delta t$$

$$s^c = U_e(t)\Delta t + a_m(\Delta t)^2\tfrac{1}{2}$$

$$\eta_e^c(t+\Delta t) = \eta_e(t) + s^c \tan\alpha$$

The iterations are continued till two successive values of $U_e^c(t+\Delta t)$ differ only by a pre-set tolerance. Thus, we see that due consideration is given to the continuous variation of velocity and acceleration at the tip during the interval Δt.

Introduction of boundary conditions in the numerical scheme

The solution system for $\dot{\eta}$ is solved after introducing the forcing upstream boundary condition (namely $\dot{\eta}$ at node 1) as below: (let $\dot{\eta}_1$ be equal to q and $C_2(1)$ the first column of

C_2; $\bar{C}_2$ represents C_2 minus the first column and first row):

$$\begin{bmatrix} 1 & \cdots 0 \cdots \\ \vdots & \\ 0 & \bar{C}_2 \\ \vdots & \end{bmatrix} \begin{Bmatrix} q \\ \dot{\eta} \end{Bmatrix} = \begin{Bmatrix} 0 \\ \bar{b}_2 \end{Bmatrix} - q \begin{Bmatrix} -1 \\ C_2(1) \end{Bmatrix}$$

At the upstream point the Galerkin equation for velocity is retained. As the downstream section is one of open boundary, it is inappropriate to prescribe the Eulerian time derivative of U. Hence, what is done is to use U_e (as explained above in the earlier part of Section 5) in the computation of the right hand side (i.e. $\{b_1\}$) while solving for U from

$$C_1\{\dot{U}\} = \{b_1\}$$

This means that the downstream boundary condition forces itself not through the time derivative of U but through prescribing U itself at that point. Thus the Galerkin equation for U is retained also at the downstream point.

6. COMPUTATION AND RESULTS

Numerical experiments were run using the model developed above. Several combinations of forcing function, bottom topography and discretizations were introduced to study the applicability. The reader is referred to Reference 15 for details of the entire set of runs. Here, the one regarding the run-up of an oscillatory incident wave is presented. The following parameters refer to the physical and numerical aspects of this run.

Still water depth = 10·0 ft; Beach slope = 0·25
Height of incident wave = 6·0 ft; wave period = 12 s
Element length = 10·0 ft; Time step = 0·06 s

Figures 10(a)–(n) depict the water profile at intervals of 0·6 s. They bring out two interesting aspects among others; one is that, just before running up the slope a steep front is formed and the other is that mild shocks run upstream as the water begins to flow on the dry area. The real world situation confirms these.

As mentioned under the moving boundary aspect the size of the end-element is time dependent. Hence, the element-matrix of this element changes with time. The corresponding portion in the global matrix is thus affected at each time step while the rest of the global matrix remains the same. In order to avoid forming the unchanging portion of the global matrix at each time step, a coupling and decoupling method was adopted for the end-element matrix with regard to the global matrix; thus only the time dependent part in the global matrix is computed at each time step. The system of linear algebraic equations is solved using a band algorithm based on Gaussian elimination. Details of this algorithm can be found in Gopalakrishnan.[15a] In the present problem the number of iterations under the Euler predictor–corrector scheme varied between 3 and 5.

Change of end-element length

The moving boundary is closely followed by letting the node at the front move with the tip of water. In this process the end-element length keeps increasing. Table I gives the element

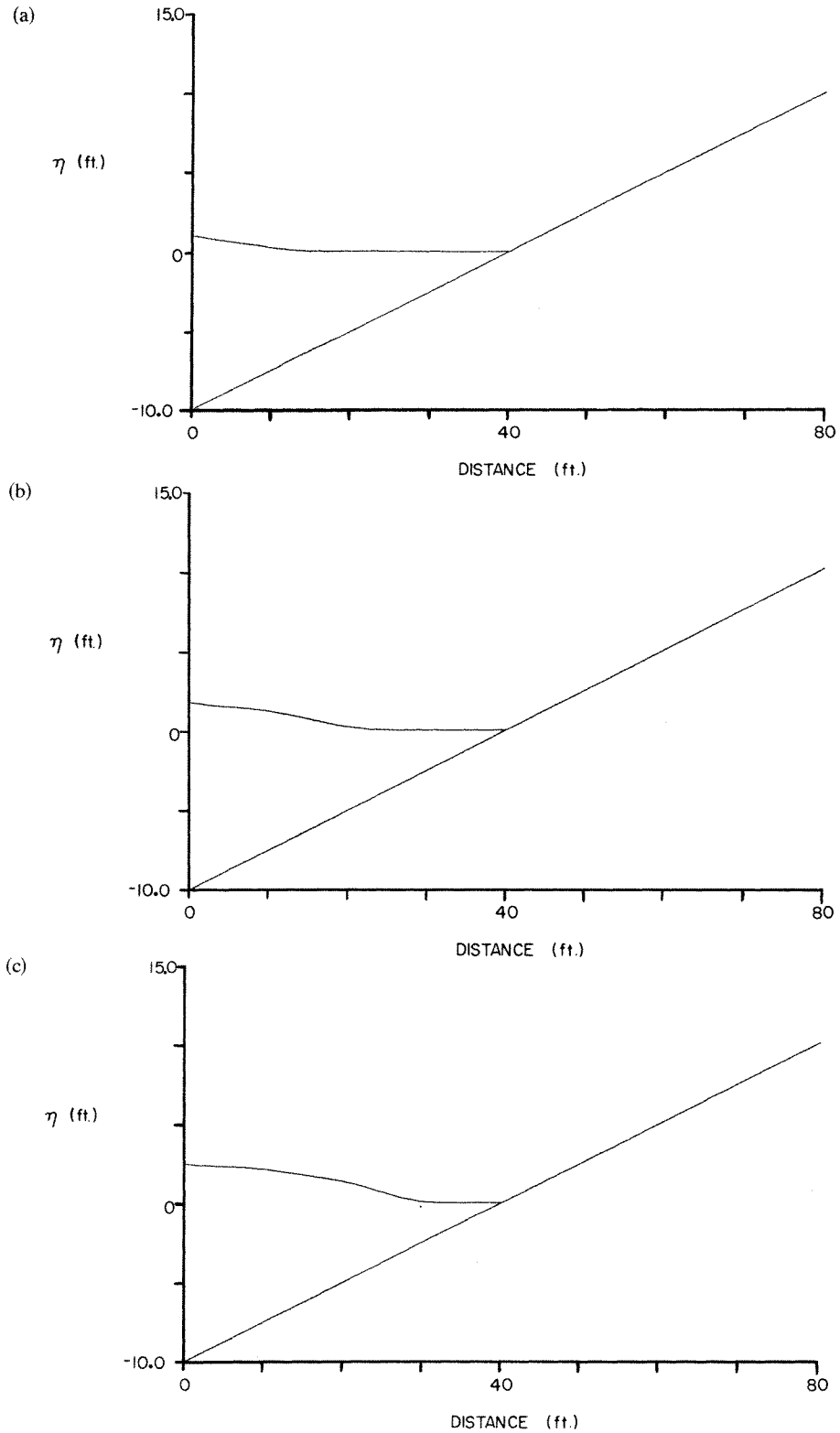

Figure 10. Run-up of oscillatory incident wave

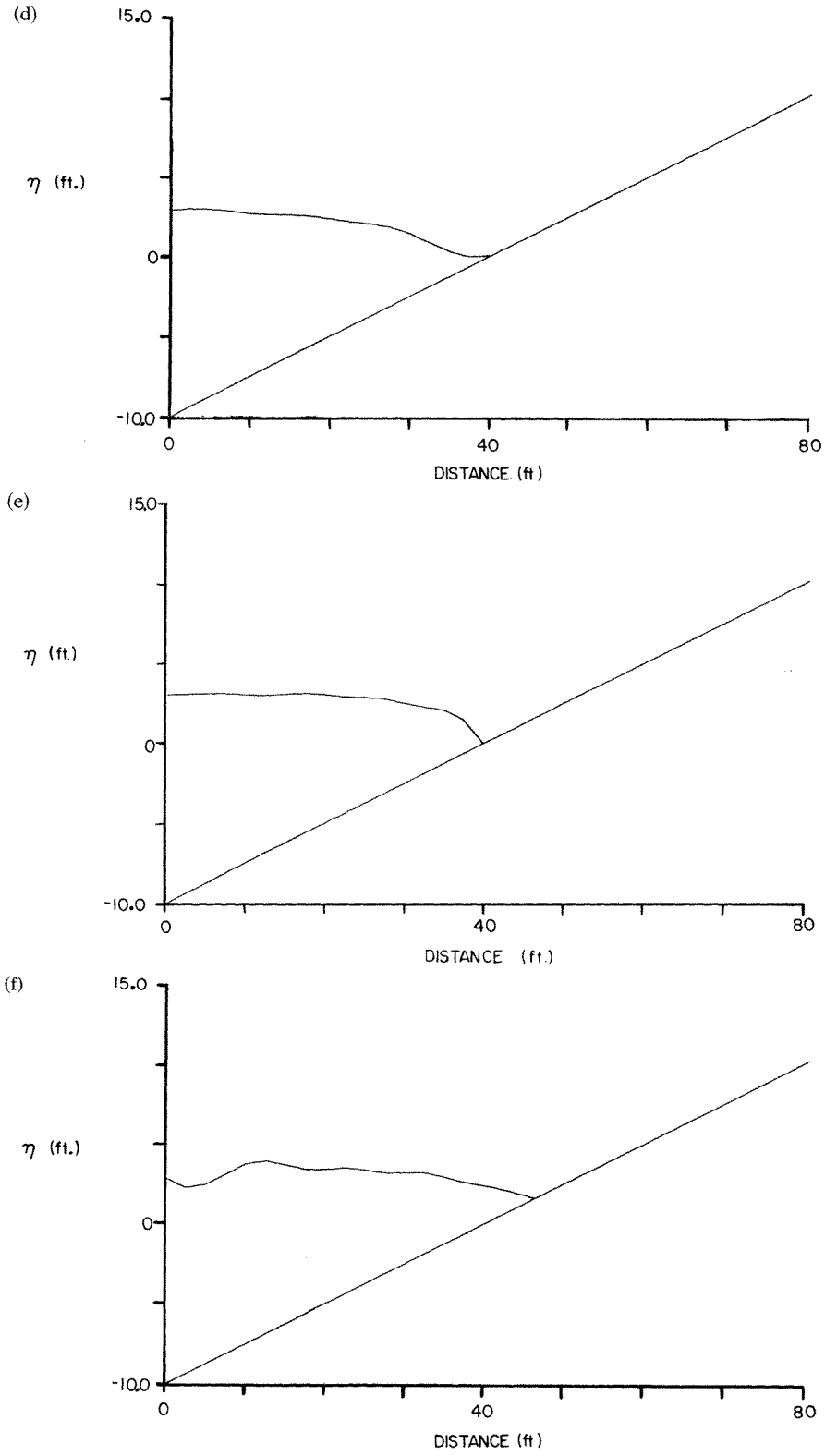

Figure 10 (*contd*)

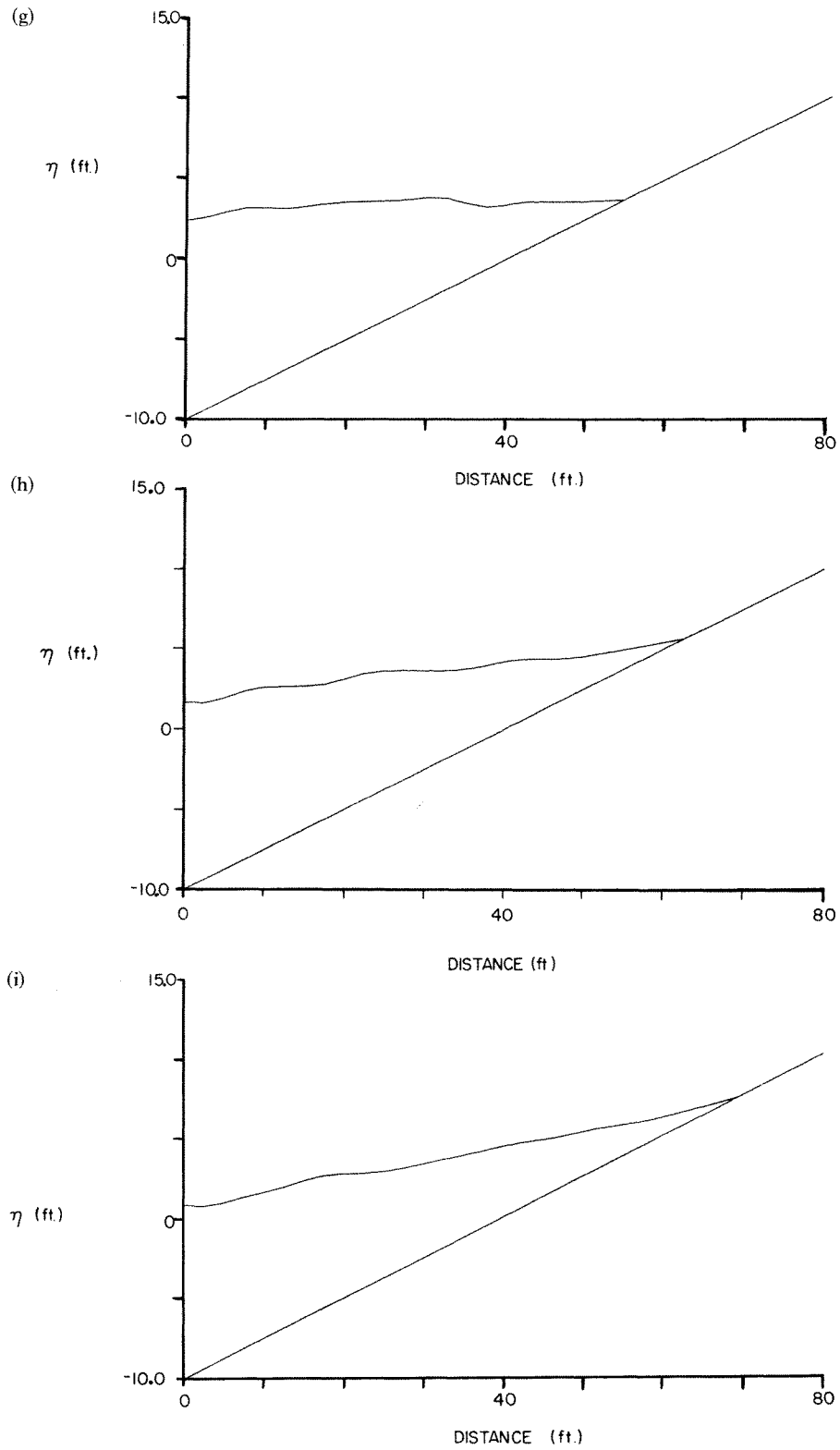

Figure 10 (*contd*)

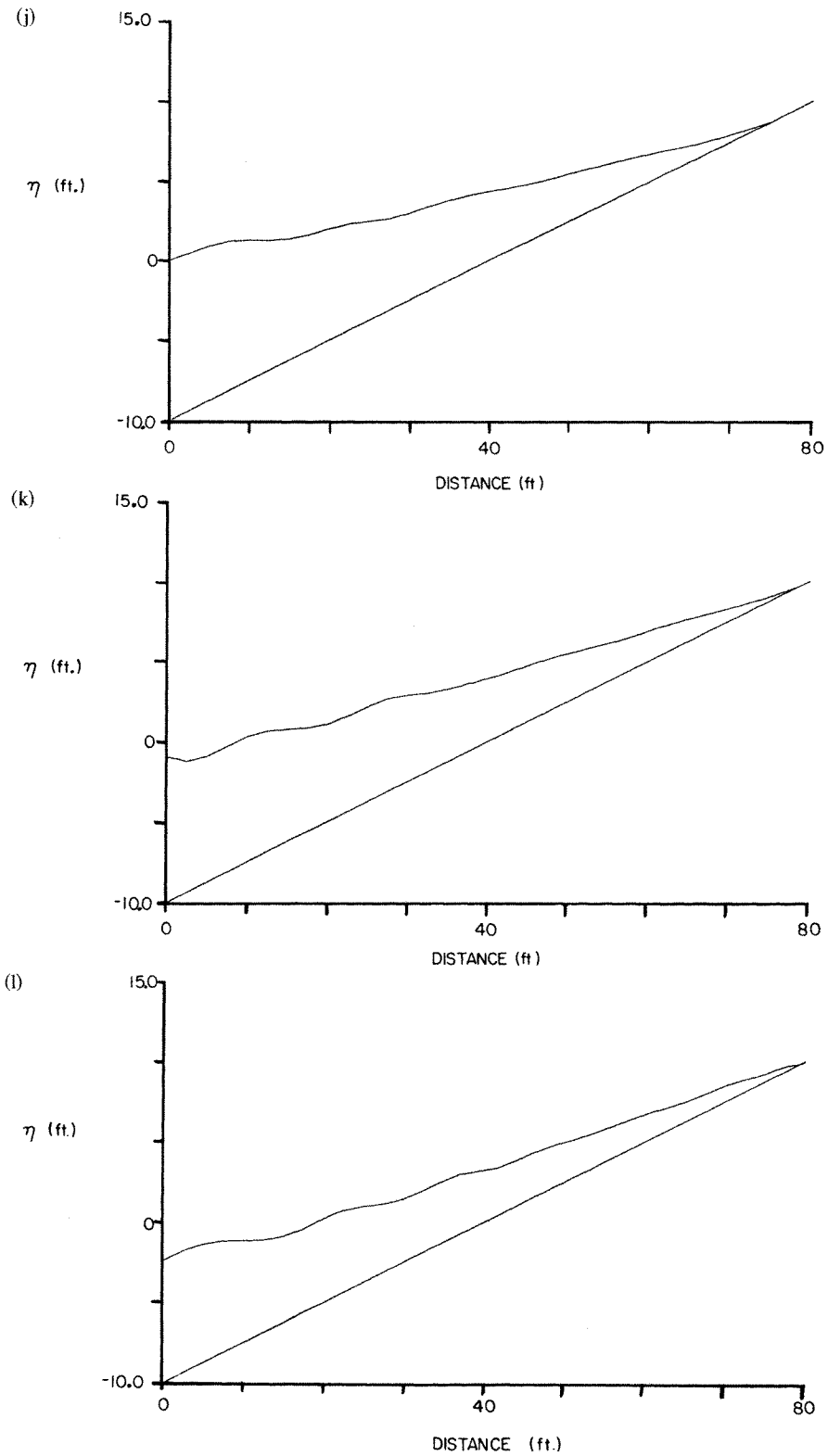

Figure 10 (*contd*)

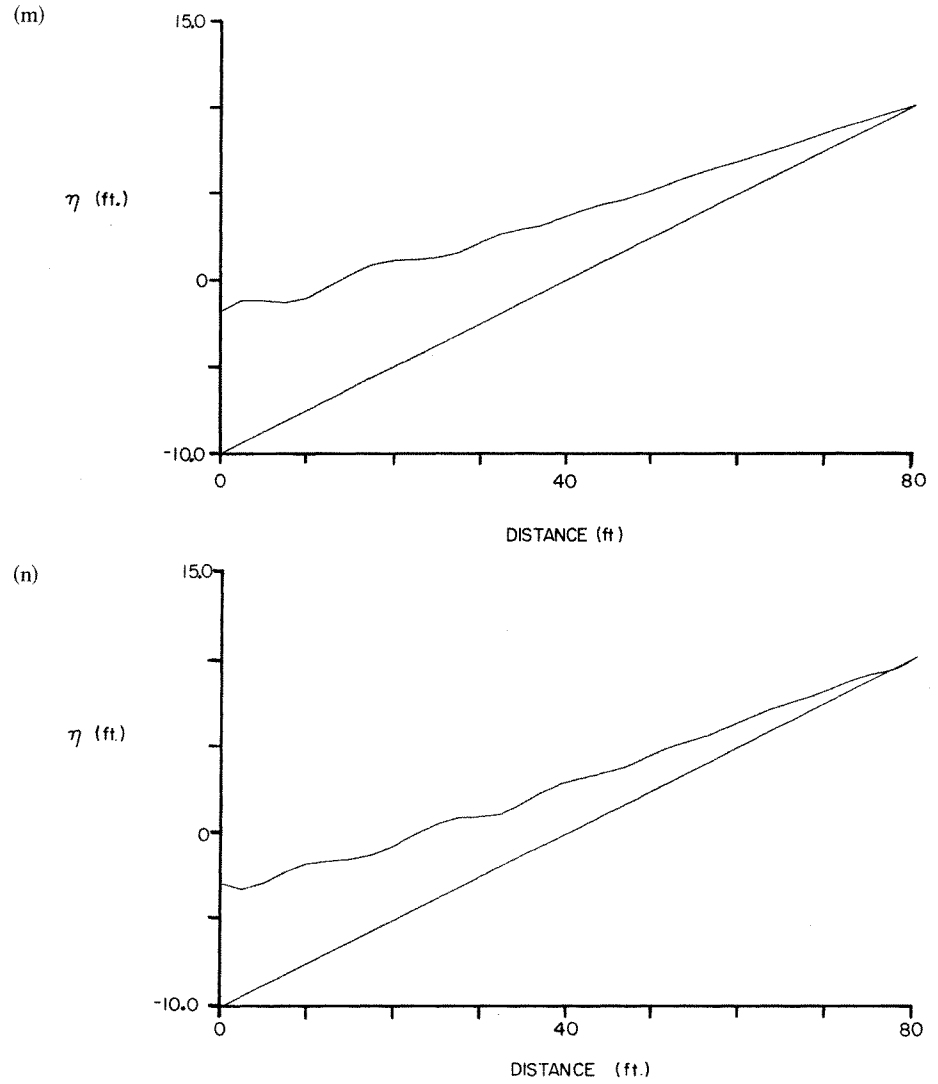

Figure 10 (*contd*)

lengths at every time step. As the end-element is split, the number of elements increases by one. It is seen that when the end-element length exceeds 1·2 times the regular length it is split such that the front element is 3 ft long and the one prior to it is 3 ft less than the end-element length just before splitting. It is also observed that the end-element shrinks first and then begins to lengthen. This indicates that the tip of the water wedge first comes down before going up the slope. Such a preliminary run-down before the phenomenon of uprush is actually observed in physical experiments. Entries in Table I relate to the following data:

Forcing function—Solitary wave of height 3 ft
Depth of water = 9 ft; Slope of beach = 0·3
Regular element length = 10 ft; Time step = 0·06 s
Initial number of elements = 3.

Table I. Element lengths (ft) at each time step

Time (s)	Element number					
	1	2	3	4	5	6
0·06	10·000	10·000	9·999			
0·12	10·000	10·000	9·993			
0·18	10·000	10·000	9·986			
0·24	10·000	10·000	9·978			
0·30	10·000	10·000	9·971			
0·36	10·000	10·000	9·966			
0·42	10·000	10·000	9·966			
0·48	10·000	10·000	9·970			
0·54	10·000	10·000	9·974			
0·60	10·000	10·000	9·973			
0·66	10·000	10·000	9·958			
0·72	10·000	10·000	9·921			
0·78	10·000	10·000	9·857			
0·84	10·000	10·000	9·767			
0·90	10·000	10·000	9·665			
0·96	10·000	10·000	9·651			
1·02	10·000	10·000	9·565			
1·08	10·000	10·000	9·681			
1·14	10·000	10·000	9·973			
1·20	10·000	10·000	10·438			
1·26	10·000	10·000	11·051			
1·32	10·000	10·000	11·775			
1·38	10·000	10·000	9·575	3·000		
1·44	10·000	10·000	9·575	3·854		
1·50	10·000	10·000	9·575	4·740		
1·56	10·000	10·000	9·575	5·647		
1·62	10·000	10·000	9·575	6·571		
1·68	10·000	10·000	9·575	7·505		
1·74	10·000	10·000	9·575	8·443		
1·80	10·000	10·000	9·575	9·381		
1·86	10·000	10·000	9·575	10·316		
1·92	10·000	10·000	9·575	11·246		
1·98	10·000	10·000	9·575	9·169	3·000	
2·04	10·000	10·000	9·575	9·169	3·913	
2·10	10·000	10·000	9·575	9·169	4·813	
2·16	10·000	10·000	9·575	9·169	5·699	
2·22	10·000	10·000	9·575	9·169	6·569	
2·28	10·000	10·000	9·575	9·169	7·421	
2·34	10·000	10·000	9·575	9·169	8·256	
2·40	10·000	10·000	9·575	9·169	9·071	
2·46	10·000	10·000	9·575	9·169	9·867	
2·52	10·000	10·000	9·575	9·169	10·644	
2·58	10·000	10·000	9·575	9·169	11·399	
2·64	10·000	10·000	9·575	9·169	9·134	3·000
2·70	10·000	10·000	9·575	9·169	9·134	3·713
2·76	10·000	10·000	9·575	9·169	9·134	4·402
2·82	10·000	10·000	9·575	9·169	9·134	5·068
2·88	10·000	10·000	9·575	9·169	9·134	5·709
2·94	10·000	10·000	9·575	9·169	9·134	6·326

Comparison of global matrices with and without end-element splitting

The entries in the global matrix corresponding to the two elements at the end are given in Figures 11 and 12 (C_2 matrix). These relate to the field conditions of the oscillatory wave mentioned before. Figure 11 corresponds to the values when the end-element splitting was adopted. Figure 12 gives the entries when such a splitting was not adopted and the end-element was allowed to continuously increase in length consistent with the moving tip. Comparing these two figures, it can be concluded that the end-element splitting retains the matrix in a balanced form and hence is necessary. The error arising out of not splitting the end element for prolonged periods is numerically shown by Gopalakrishnan.[15a]

One of the questions that would arise is regarding the significance of the vertical accelerations; in other words, do they contribute substantially to justify their inclusion? In order to investigate this issue, numerical runs were made, alternately including and excluding vertical accelerations for the run-up of waves with two different steepnesses and two different bottom slopes. The results indicated certain interesting features. On comparing the

7·43	0·00	1·28	−3·10		
0·00	18.80	3·10	−7·20	0·00	
1·28	3·10	7·43	0·00	1·28	−3·10
−3·10	−7·20	0·00	18·80	3·10	−7·20
	0·00	1·28	3·10	3·72	−4·71
		−3·10	−7·20	−4·71	9·40

(a)

6·80	0·01	1·18	−2·60		
0·01	14·43	2·60	−5·54	0·00	
1·18	2·60	5·71	−2·14	0·80	−1·20
−2·60	−5·54	−2·14	9·48	1·20	−1·73
	0·00	0·80	1·20	2·31	−1·82
		−1·20	−1·73	−1·82	2·26

(b)

Figure 11. Matrix elements with end-element splitting: (a) $t = 1{\cdot}0$ s; (b) $t = 6{\cdot}0$ s

7·43	0·00	1·28	−3·10		
0·00	18·80	3·10	−7·20	0·00	
1·28	3·10	19·83	83·85	5·57	−58·28
−3·10	−7·20	83·85	775·34	56·28	−586·89
	0·00	5·57	58·28	16·11	−88·56
		−58·28	−586·89	−88·56	765·94

Figure 12. Matrix elements without end-element splitting: $t = 6{\cdot}0$ s

run-up values with the experimental values presented by Horikawa[17a] it is seen that the model with the vertical accelerations produced correct results while the one without them indicated a 50 per cent higher run-up. Another aspect is that the model with the acceleration effects predicted the inception of the wave breaking systematically whereas the other model did not do so. In fact, such a lapse seems to be serious because in one numerical run (with the vertical accelerations not included) the run-up was 2·5 times the corresponding experimental value!

CONCLUSION

A numerical model based on the Galerkin finite element procedure has been developed to resolve a moving boundary coastal problem. The present study also includes a way to introduce the effects of vertical accelerations in the one-dimensional momentum equation. The model and the theory combine to work well and (as indicated in Reference 15) reproduce the physical phenomenon of wave run-up with a high degree of accuracy.

The present model can handle only situations where waves do not break. It has been observed in nature that waves do climb without breaking if the slope of the beach is moderately or very steep—such as 1 on 5 or steeper. However, for very steep slopes the governing equations developed in this study become inapplicable because some of the assumptions made therein no longer hold true. Under such circumstances a 2-D model is warranted. The same concepts of tackling the moving boundary as indicated in this study can be used for the 2-D model except that the Lagrangian accelerations should be considered now for all nodes on the free surface. Preliminary results of this have been obtained and further work will be published separately.

ACKNOWLEDGEMENT

This work was part of the doctoral thesis of the first author. Assistance of the then Center for Marine and Coastal Studies, NCSU, Raleigh, NC, is gratefully acknowledged.

REFERENCES

1. K. J. Bathe, J. T. Oden and W. Wunderlich, (eds.), *Formulations and computational Algorithms in Finite Element Analysis: US–Germany Symposium*, MIT, Cambridge, Mass., 1977.
2. P. L. Betts, 'A variational principle in terms of stream function for free-surface flows and its application to the finite element method', *Computers and Fluids*, **7**, 145–153 (1979).
3. B. A. Boley, 'An applied overview of moving boundary problems', in Reference 40.
4. R. Bonnerot and P. Jamet, 'A second order finite element method for the one-dimensional Stefan problem', *Int. J. Numer. Math. Eng.* **8**, 811–820 (1974).
5. R. Bonnerot and P. Jamet, 'Numerical computation of the free boundary for the two-dimensional Stefan problem by space-time finite elements, *J. Comput. Phys.*, **25**, 163–181 (1977).
6. J. P. Boris, K. L. Hain and M. J. Fritts, *in Proceedings, First Int. Conference on Numerical Ship Hydrodynamics*, David W. Taylor, Naval Ship R&D Center, Bethesda, Md., 1975.
7. S. T. K. Chan, B. E. Lerock and L. R. Herrmann, 'Free surface ideal fluid flows by finite elements', *J. Hydraulics Div., ASCE*, **99**, 959–974 (1973).
8. J. J. Connor and C. A. Brebbia, *Finite Element Techniques for Fluid Flow*, Newnes–Butterworth, London, 1976.
9. J. Crank, 'Finite-difference methods' in Reference 27.
10. C. S. Desai, 'Finite elements for flow problems in porous media' R. H. Gallagher *et al.* (eds.) in *Finite Elements in Fluids* 1, Wiley, Chichester, 1975.
11. C. M. Elliott and V. Janovsky, 'A finite element discretization of a variational inequality formulation of a Hele-Shaw moving boundary problem, in (ed.) J. R. Whiteman *MAFELAP 1978*, Academic Press, London, 1979.
12. G. J. Fix, 'A survey of numerical methods for selected problems in continuum mechanics', in *Numerical Models of Ocean Circulation*, National Academy of Sciences, Washington D.C., 1975.

13. L. Fox, 'What are the best numerical methods?', in Reference 27.
14. P. W. France, 'A simple technique for the analysis of free surface flow problems', *Advances in Water Resources*, **4,** 20–22 (1981).
15. T. C. Gopalakrishnan and C. C. Tung, 'Run-up of non-breaking waves—a finite element approach', *Coastal Engineering* **4,** 3–22 (1980).
15a. T. C. Gopalakrishnan, 'Galerkin finite element analysis of wave shoaling and run-up', *Doctoral thesis*, Center for Marine and Coastal Studies, North Carolina State Univer., NC 27650, USA, 1978.
16. K. L. Heitner and G. W. Housner, 'Numerical model for tsunami run-up', *J. Waterways Harbours Div. ASCE*, **96,** WW3, 701–719 (1970).
17. K. P. Holz and D. Withum, in Reference 1.
17a. Horikawa, K., *Coastal Engineering*, Wiley, New York, 1978.
18. M. Ikegawa and K. Washizu, 'Finite element method applied to analysis of flow over a spillway crest, *Int. J. Numer. Meth. Eng.* **6,** 179–189 (1973).
19. P. Jamet and R. Bonnerot, 'Numerical solution of the Eulerian equations of compressible flow by a finite element method which follows the free boundary and the interfaces', *J. Comput. Phys.*, **18,** 21–45 (1975).
20. J. J. Leendertse, 'A water-quality simulation model for well-mixed estuaries and coastal seas': Vol. I. *Principles of Computation*, RM-6230-RC, The Rand Corporation, Santa, Monica, California, 1970.
21. D. R. Lynch and W. G. Gray, 'Finite element simulation of flow in deforming regions', *J. Comput. Phys.* **36** (2), 135–153 (1980).
22. D. R. Lynch, Discussion on Reference 43, *J. Waterway, Port, Coastal and Ocean Div. ASCE*, **106,** WW3, 425–428 (1980).
23. D. R. Lynch and K. O'Neill, 'Continuously deforming finite elements for the solution of parabolic problems, with and without phase change; *Int. J. Numer. Meth. Eng.*, **17,** 81–96 (1981).
24. G. H. Meyer, 'The numerical solution of multi-dimensional Stefan problems', in Reference 40.
25. M. Mori, 'A finite element method for solving moving boundary problems', *Int. Federation for Information Processing Conference on Modeling of Environmental Systems*, Tokyo, 167–171, 1976.
26. Y. Nakano, 'Theory and numerical analysis of moving boundary problems in the hydrodynamics of porous media', *Water Resources Research*, **14** (1), 125–134 (1978).
27. J. R. Ockendon and W. R. Hodgkins, (Eds.), *Moving boundary Problems in Heat-flow and Diffusion*, Oxford University Press, (Clarendon), Oxford, 1975.
28. T. W. Patten and B. A. Finlayson, 'Finite element methods for visco-elastic fluids', *Fundamental Research in Fluid Mechanics*, AIChE 70th Annual Meeting, New York, NY, 1977.
29. B. R. Pearce, 'Numerical calculations of the response of coastal waters to storm systems', *Tech. Report No. 12*, Coastal and Oceanographic Engineering Lab., Univ. of Florida, Gainesville, Fla., 1972.
30. D. H. Peregrine, 'Long waves on a beach', *J. Fluid Mech.*, **27** (4), 815–827 (1967).
31. G. F. Pinder and W. G. Gray, *Finite Element Simulation in Surface and Subsurface Hydrology*, Academic press, New York, 1977.
32. R. O. Reid and B. R. Bodine, 'Numerical model for storm surges in Galveston Bay', *J. Waterways Harbours Div. ASCE* **94,** WW1, 33–57 (1968).
33. L. I. Rubinstein, 'The Stefan problem', *Transactions of Mathematical Monographs*, **27,** American Math. Soc., Providence, R.I., 1967.
34. K. J. Rushchak, 'A method for incorporating free boundaries with surface tension in finite element fluid-flow simulators', *Int. J. Numer. Math. Eng.*, **15,** 639–648 (1980).
35. C. Taylor and J. Davis, 'Tidal and long wave propagation—a finite element approach', *Computers and Fluids*, **3,** 125–148 (1975).
36. R. L. Taylor and C. B. Brown, 'Darcy flow solutions with a free surface', *J. Hydraulics Div. ASCE*, **93,** HY2, 25–33 (1967).
37. E. Varoglu and W. D. Liam Finn, 'Variable domain finite element analysis of free surface gravity flow', *Computers and Fluids*, **6,** 103–114 (1978).
38. R. Walton and B. A. Christensen, 'Friction factors in storm surges over inland areas', *J. Waterway, Port, Coastal and Ocean Eng. Div. ASCE*, **106,** WW2, 261–271 (1980).
39. J. J. Wanstrath, 'Storm surge calculations in transformed coordinates', *Thesis presented to Texas A&M University*, College Station, Texas (1975).
40. D. G. Wilson, A. D. Solomon and P. T. Boggs, *Moving Boundary Problems*, Academic Press, New York, 1978.
41. T. Xanthopoulos and C. Koutitas, 'Numerical simulation of a two-dimensional flood wave propagation due to dam failure', *J. Hydraulic Res.*, **14** (4), 321–331 (1976).
42. G. T. Yeh and F. F. Yeh, 'A generalized model for storm surges', *Proc. 15th Int. Conf. Coastal Eng.*, **1,** Ch. 54, 921–933 (1976).
43. G. T. Yeh and F. K. Chou, 'Moving boundary numerical surge model', *J. Waterway, Port, Coastal and Ocean Eng. Div. ASCE*, **105,** WW3, 247–263 (1979).
44. G. T. Yeh and F. K. Chou, Reply to Discussion, *J. Waterway, Port, Coastal and Ocean Eng. Div. ASCE*, **107,** WW1, 34–36 (1981).
45. O. C. Zienkiewicz, *The Finite Element Method in Engineering Science*, McGraw Hill, New York, 1971.